SOFT ROBOTS

OmniSkins: Robotic skins that turn inanimate objects into multifunctional robots

Joran W. Booth[1], Dylan Shah[1], Jennifer C. Case[1,2], Edward L. White[2], Michelle C. Yuen[1,2], Olivier Cyr-Choiniere[1], Rebecca Kramer-Bottiglio[1]*

Robots generally excel at specific tasks in structured environments but lack the versatility and the adaptability required to interact with and locomote within the natural world. To increase versatility in robot design, we present robotic skins that can wrap around arbitrary soft bodies to induce the desired motions and deformations. Robotic skins integrate actuation and sensing into a single conformable material and may be leveraged to create a multitude of controllable soft robots with different functions or gaits to accommodate the demands of different environments. We show that attaching the same robotic skin to a soft body in different ways, or to different soft bodies, leads to distinct motions. Further, we show that combining multiple robotic skins enables complex motions and functions. We demonstrate the versatility of this soft robot design approach in a wide range of applications—including manipulation tasks, locomotion, and wearables—using the same two-dimensional (2D) robotic skins reconfigured on the surface of various 3D soft, inanimate objects.

INTRODUCTION

Robots are typically designed to perform a finite collection of tasks in a known context. This approach produces efficient solutions when the environment is structured and predictable. However, in many situations—such as exploration, search and rescue, or operating alongside humans—knowledge of the task to be performed, or the context in which it is to be performed, cannot be known a priori. One approach to alleviating this problem is the use of soft materials in robotics (*1*–*3*), where material deformation both enables damage-resilient soft robots (*4*) and allows simple designs to extend to multiple motion patterns (*5*). Soft robots have been shown to be advantageous for manipulation of delicate objects (*6*, *7*), compliance-matched for wearability (*8*–*10*), and able to withstand large impact forces (*11*, *12*). Soft robots have also been shown to achieve multiple locomotion gaits with the same structure, such as crawling and undulation of elastomeric robots (*5*, *13*) and hopping and rolling of spherical robots (*14*, *15*). Another soft robot was shown to perform both locomotion and grasping tasks (*16*). Multifunctionality in soft robots may be further enabled by modular and reconfigurable systems (*13*, *17*, *18*).

We introduce a soft robot design approach based on active robotic skins that manipulate soft, deformable bodies from their surface. Robotic skins are modular, conformable sheets with embedded sensing and actuation, which may be applied to, removed from, transferred between, and reoriented on the surface of soft bodies (e.g., inflatables, foams, and limbs) to impart motion onto those bodies. This surface-based approach allows any passive soft object to be turned into an active soft robot (Fig. 1). Three principles enable multifunctional robot design with this approach: First, distinct motions may be achieved by reorienting a robotic skin on the surface of a soft body. Second, distinct motions may be achieved by wrapping a robotic skin around bodies with different properties and/or morphologies. Third, multiple robotic skins may be used in combination and reconfigured to perform different tasks. We demonstrated sensor-enabled closed-loop control of the robotic skins independent of specific actuator and substrate material choices. We further demonstrated transferability of the robotic skins between soft bodies to accomplish a wide variety of tasks, including an inchworm robot that was controlled either remotely by an operator or with onboard light sensors, a continuum manipulator that grasped and moved objects, an upper-body wearable garment that communicated posture information to a user, and a tensegrity structure that was surface-actuated using the robotic skins.

RESULTS

Design of robotic skins

Robotic skins are two-dimensional (2D), fully controllable robotic systems that can deform soft objects from their surface. The objective of this work is to demonstrate the merits of this surface-based approach, without confining the concept to any one particular implementation. A large design space exists for robotic skins, which includes variation in components (actuators, sensors, and substrates), configuration (layout of components and geometry of the skin), and level of component integration. As examples, we fabricated three implementations of robotic skins.

To show that different components can be used, we fabricated two implementations in a simple parallel component configuration but with different actuators and substrates. One of the implementations used pneumatic actuators integrated into an elastomer substrate (*8*), whereas the other used coiled shape memory alloy (SMA) actuators integrated onto a fabric substrate (*19*–*21*). Both implementations used conductive composite–based capacitive sensors (*22*). Because actuator choice dominates the overall performance of a robotic skin system, we refer to these two implementations as pneumatic skins and SMA skins.

To show that different configurations can be used, we fabricated a third implementation in a triangular component configuration. This implementation included pneumatic actuators, a fabric substrate, and the same capacitive sensors. Triangulation of actuators produced biaxial strains and therefore accommodated compound

[1]School of Engineering and Applied Science, Yale University,10 Hillhouse Avenue, New Haven, CT 06520, USA. [2]School of Mechanical Engineering, Purdue University, 585 Purdue Mall, West Lafayette, IN 47907, USA.
*Corresponding author. Email: rebecca.kramer@yale.edu

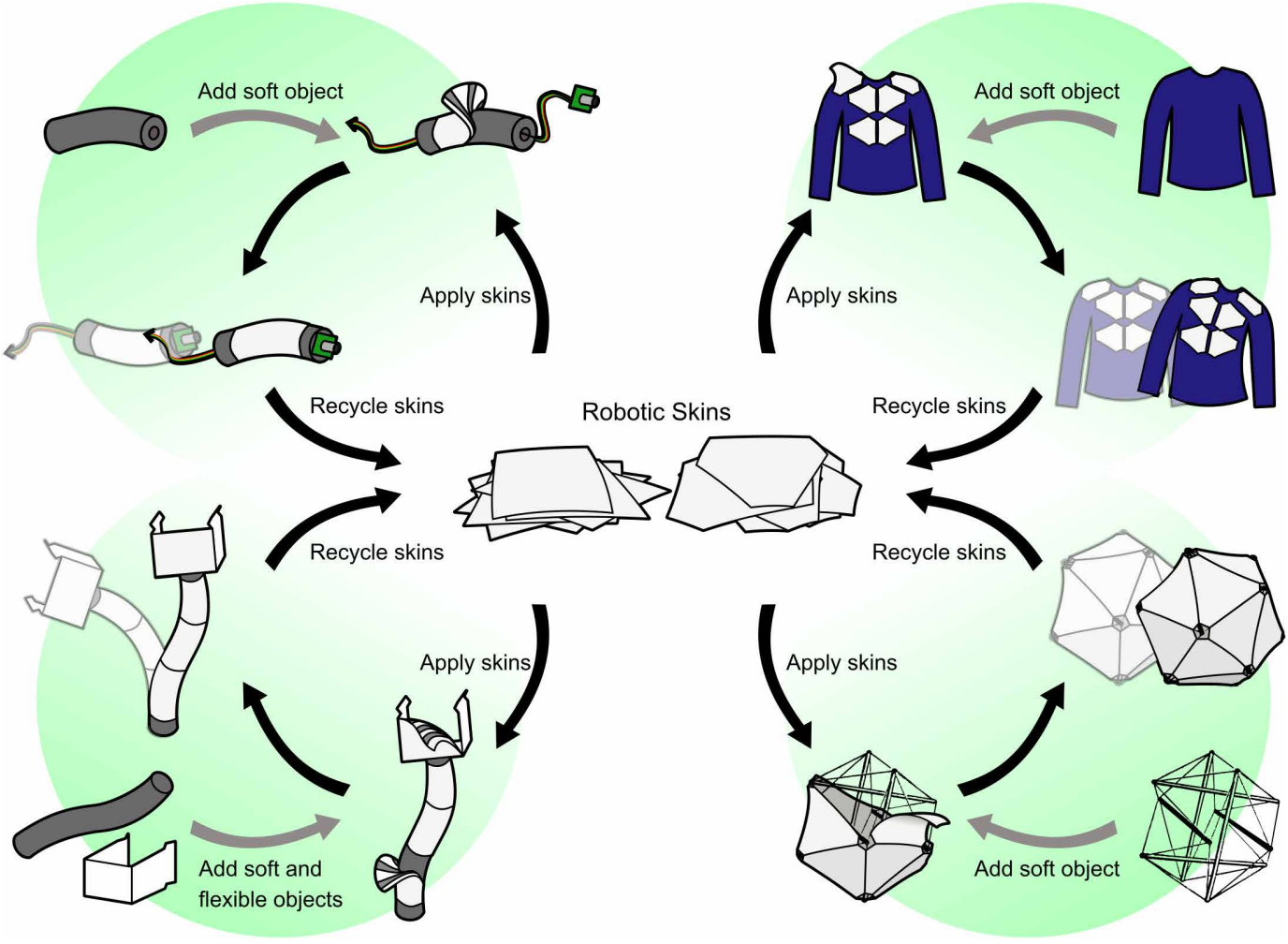

Fig. 1. Surface-based modular robots can turn any soft body into a robotic system. A robotic skin is a modular, 2D soft robot that can be reconfigured on the surface of passive, deformable bodies to produce deformations. Robotic skins can be assembled around different soft bodies in different orientations to produce a wide range of robotic systems. This class of robots holds potential for applications where operators need highly reconfigurable, lightweight robots to assist in variable tasks.

curvature host bodies, whereas parallel actuators produced uniaxial strains and accommodated simpler, single curvature host bodies. Other possible configurations include multiple robotic skins that could be overlaid or other nonparallel actuator layouts, such as radial patterns or Cartesian grids. Further information on the materials, dimensions, and manufacture of the robotic skins can be found in Materials and Methods and in the Supplementary Materials.

Reorienting robotic skins on a soft body enabled distinct motions

The first demonstrated principle of operation is that a robotic skin may be used in combination with a soft, deformable body, where attaching the same robotic skin to a soft body in different ways leads to distinct motions. We show a simple example of this principle by using a robotic skin with integrated actuation and sensing attached to a cylindrical foam body. By orienting the actuators along the length of the cylinder, linear contraction induced bending motion; by reorienting the actuators orthogonally, radial contraction induced compression (Fig. 2). Other motion primitives include axial extension, axial contraction, and torsion.

Placing a robotic skin on different soft bodies affected motion

The second principle we demonstrated is that using the same skin on soft bodies with different dimensions and mechanical responses yielded different motions. The motion achieved depends on the relationship between the dimensions, material properties, and force capabilities of the skin and the dimensions and stiffness characteristics of the body. We can leverage this codependence of the motion on both the skin's capabilities and the body's mechanical properties to create a variety of motions by reusing the same robotic skin. This concept is appealing because changing out the soft body to adjust the robot's motion is often much simpler than altering the robotic components (actuators, sensors, and controllers).

As an example, we focused on a continuum bending motion. By wrapping the same robotic skin around cylindrical foam bodies with different radii, we achieved different maximum deflections or workspaces. A robotic skin wrapped around a soft cylinder induced more deflection as the radius of the host cylinder decreased (Fig. 3), assuming homogeneous material properties and constant curvature

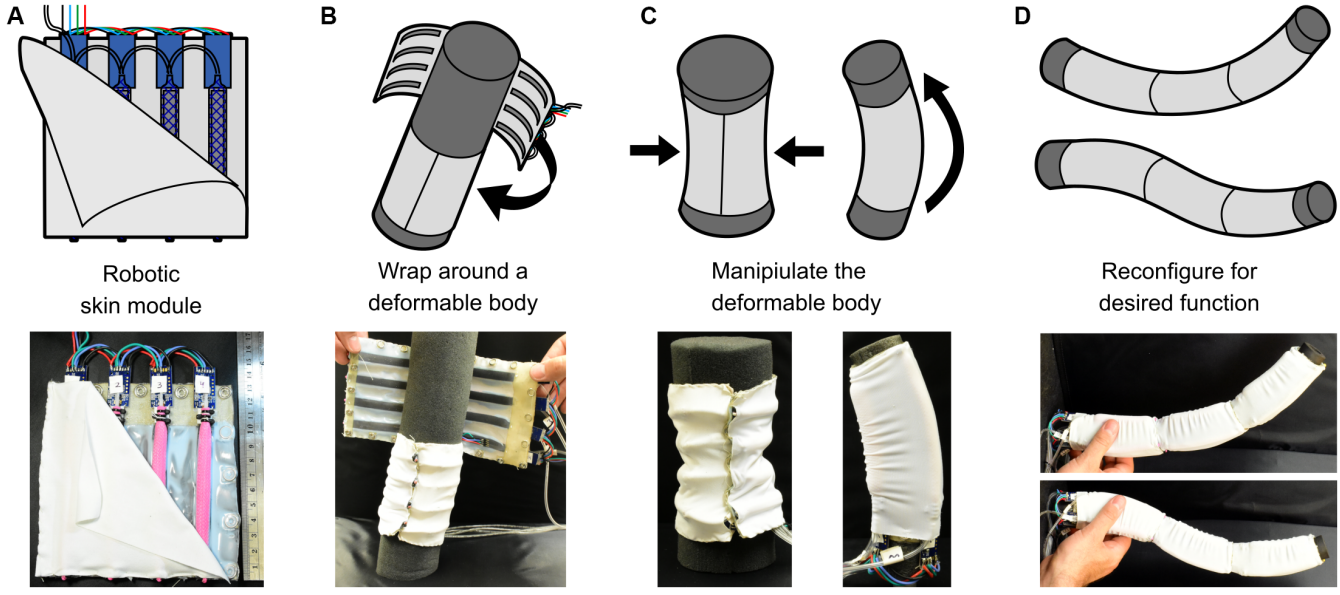

Fig. 2. Operational concept. (**A**) Robotic skins embed distributed actuation and sensing into a conformable substrate. (**B**) Robotic skins may be wrapped around soft bodies to impart motion onto those bodies. (**C**) Robotic skins may be reoriented on a soft body to produce different forms of motion. (**D**) Multiple robotic skins can be combined into larger assemblies to produce complex motions.

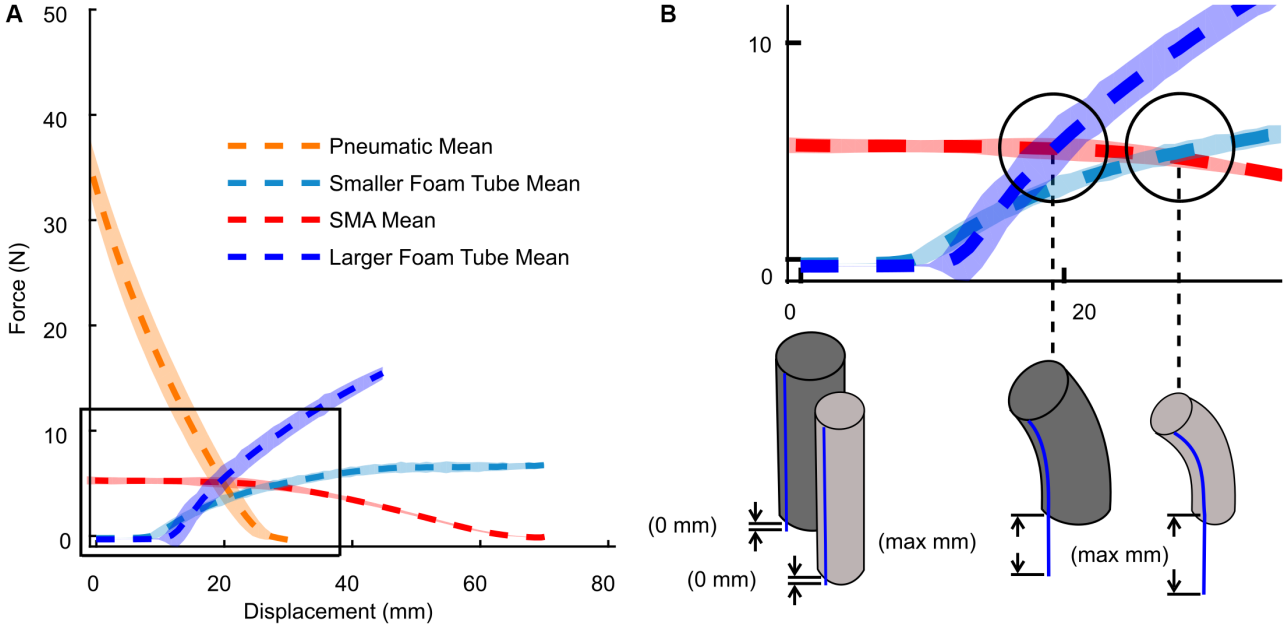

Fig. 3. Robotic skins perform differently on different soft bodies. Here, soft cylinders of different radii will yield different maximum deflections (workspaces) for a bending segment. (**A**) By comparing the blocked force of the robotic skin actuators with the force required to deflect the soft cylinder, the maximum deflection may be predicted. The equilibrium points are highlighted in (**B**). Shaded regions around the means represent 95% confidence intervals.

(*23*). Further, by comparing the blocked force characteristics of a contraction actuator with the force required to deform the cylinder, we could predict the maximum deflection of the system. Figure 3A plots these forces for both the pneumatic and SMA actuators used in our implementations, as well as two foam cylinders with radii of 31.75 mm (1.25 in) and 44.45 (1.75 in). Figure 3B shows the intersections of the force curves, which indicate the maximum deflections achievable when pairing specific actuators with specific soft bodies. In our case, displacements of 27.4 mm (41.4° deflection) and 19.2 mm (29.3° deflection) were predicted for SMA actuators paired with the smaller and larger radius cylinders, respectively.

The above case highlights how a skin-body system can be designed to achieve a desired deformation. However, the skins may also be used on arbitrary soft bodies where the material properties are not known beforehand. Further details on the theoretical basis for predicting the deformation of bending systems composed of robotic skins and soft bodies with both known and unknown properties can be found in the Supplementary Materials.

Reconfiguring robotic skins and soft bodies enabled multifunctionality

The third principle that we demonstrated is that multiple robotic skins may be used in combination to produce more complex motions and reconfigured for variable tasks (Fig. 4). After completing a task in one configuration, robotic skins can be removed and transferred to a different body to accomplish a different task. We demonstrated a simple case of this transferability by reconfiguring three robotic skins in combination with various cylindrical foam bodies to achieve three distinct functions. First, the skins were connected in series on a long foam body to create a multisegment continuum robot (Fig. 4, A to B). Second, the skins were separated and applied to new deformable bodies to produce different locomotion gaits (Fig. 4, C to H). Third, the skins were applied to a three-fingered end effector to demonstrate grasping (Fig. 4, I to L). These functions—continuum motion, locomotion, and grasping—were selected because they are often the building blocks used in complex robotic systems and can be leveraged to achieve a wide range of combinatorial tasks.

Multisegment continuum robot

By leveraging the bending motions previously described, multiple robotic skins can work in collaboration on a single body to achieve more complex motions. We demonstrated this by using three skins positioned on a long foam cylinder to form a three-segment continuum robot (Fig. 4, A and B). Design considerations, such as the number of skins and distance between them, may easily be modified, as well as the individual performance of each segment of the continuum robot system by using robotic skins with different actuators if desired.

Locomotion robots

The robotic skins are capable of producing many modes of locomotion. Here, we show three different gaits achieved by the pneumatic skins: rowing, inchworm, and bodiless inchworm. Additional gaits are presented in the Supplementary Materials. For all locomotion gaits demonstrated in Fig. 4, the actuators were pressurized at convenient rates (between 3 and 10 Hz) and pressures (140 kPa). The rowing gait was generated by attaching a skin to a foam cylinder with weighted end caps and cycling through the actuators (Fig. 4, C and D). Locomotion inspired by the inchworm (*24*, *25*) was achieved by wrapping a skin around a foam cylinder with polystyrene "feet" on the ends (Fig. 4, E and F). We further generated a bodiless inchworm gait, which demonstrates that robotic skins with components tightly integrated into the substrate may operate independently of a host body (Fig. 4, G and H). To achieve bodiless inchworm locomotion, we simultaneously and cyclically contracted and then relaxed all of the skin's actuators, resulting in repeated arching and flattening of the skin, and forward motion due to biased feet. In all cases,

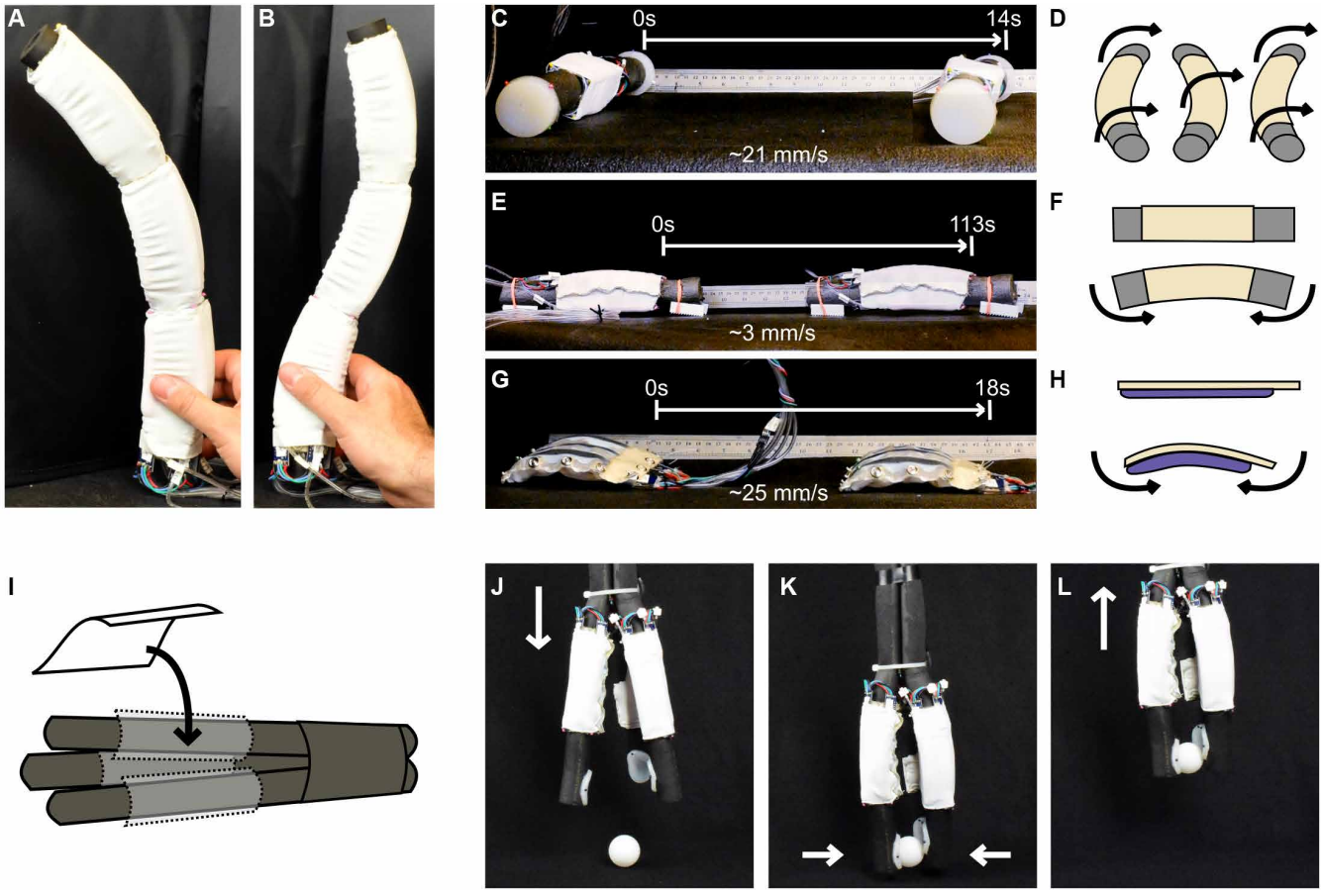

Fig. 4. Modular robotic skins can be combined and/or reconfigured for various tasks. (**A** and **B**) Three robotic skins are linked together to form a continuum robot. These are then separated into three individual robotic skin modules and used to generate different locomotion gaits: (**C** and **D**) rowing locomotion, (**E** and **F**) inchworm locomotion, and (**G** and **H**) bodiless inchworm locomotion. (**I** to **L**) The three robotic skins are then transferred to a three-fingered grasping end effector, using one robotic skin per finger.

the locomotion gait and speed may be modified by tuning the skin-body interaction or parameters of the skin itself.

Grasping end effector

We further used the same robotic skins previously used for the three-segment continuum robot and three locomotion robots to demonstrate a three-fingered grasping end effector (Fig. 4, I to L). The skins were attached to foam cylinders bundled together, and high-friction pads were applied to each fingertip to increase contact friction with objects. To achieve the grasping motion, each skin bent its cylinder inward to grasp the object.

Closed-loop control of robotic skins

We demonstrated sensor feedback and closed-loop control of systems using robotic skins (Fig. 5). In our implementations, we controlled the robotic skins by pairing each actuator with an off-board pressure or current controller and each sensor with an onboard signal conditioning circuit. Sensors and actuators were colocated in pairs and can be used to provide direct state feedback, rather than relying on inferential measures such as pressure or motion capture. This direct measurement approach has been enabled by recent advances in large-deformation strain-sensing technologies (*26*, *27*). The sensors used in our implementations were made from a silicone composite that relies on expanded intercalated graphite (EIG) to achieve electrical conductivity (*22*). We used this conductive composite as the electrode material to fabricate high-deformation capacitive strain sensors with a linear relationship between capacitance and length (see fig. S8C). Sensor outputs during open-loop inchworm locomotion for both pneumatic and SMA skins are shown in Fig. 5 (A and B).

The sensor information can be used to create sense-plan-act loops. To demonstrate these loops, we wrapped both the pneumatic and the SMA skins around a foam cylinder with a 31.75-mm (1.25-in) diameter. By controlling a single actuator, the robot was commanded to shorten one side of the body in a stair-step pattern (Fig. 5, C and D). We were able to consistently control the change in length of one side of the cylinder to a resolution of 1 mm, with an initial sensor length of 90 mm, with both types of skins.

The pneumatic skin had its sensors bonded to its contraction-type McKibben actuators (which start in their extended, strain-limited state), and thus, its sensors can only contract. In contrast, the sensors in the SMA skin were not strain-limited by their corresponding actuators. When the SMA skin bent a deformable body, the sensor on the outer surface of the curved body was fully pressed against the body, therefore giving a reliable measure of the strain in the underlying surface. Therefore, in Fig. 5C, we plot the pneumatic skin's set point as a contraction (the skin using an actuator to contract its underlying sensor), whereas in Fig. 5D, we plot the SMA skin's set point as an extension (the skin using an actuator to stretch its opposing sensor).

Because we measured the deformation of the surface of a body, our control algorithm was not dependent on the material or the dimensions of the underlying deformable body. Rather, the linear response of the sensors was used to infer the length of the underlying portion of the skin. For the SMA skin, we implemented a bang-bang control algorithm. For the pneumatic skin, a proportional-integral controller was used as an additional control loop to deal with the faster dynamics of the pneumatic system. The complete actuation time of the pneumatic actuators was on the order of 20 ms, relative to an actuation time of a few seconds for the SMA actuators. The actuator dynamics are detected by the sensors, which have a sample time on the order of 4 ms. Further information about the control algorithms can be found in the Supplementary Materials.

Applications and comparisons to purpose-built systems

Because robotic skins are modular (combinable and separable), reconfigurable (easily removed from, transferred between, and reoriented on host bodies), and fully controllable, they could be used to "roboticize" a wide variety of soft objects to achieve variable tasks (see Fig. 6 and movies S1 to S6). Single skins could be used for locomotion robots and may be integrated with other elements to create a complex robotic system. For example, we used a skin affixed to a foam cylinder to create an inchworm robot and further added either a camera or light sensors to achieve control by a teleoperator or control by external light (Fig. 6A). In another demonstration, we used robotic skins to create continuum manipulators (Fig. 6B), with different orientations of the skins being useful for different types of end effectors (movies S1 to S6). Given the planar, conformable nature of robotic skins, they also lend well to wearable applications. We demonstrated this by affixing robotic skins to an upper-body garment. Sensors in the skins detected the posture of the wearer and communicated poor posture (above a sensor output threshold) by pulsing the actuators gently, creating a user-in-the-loop control scheme (Fig. 6C). Last, the robotic skins could be combined with complex geometries, such as a six-bar passive tensegrity structure (an icosahedron). We used 20 triangular robotic skins, which were also used in the wearable demonstration and attached at the vertices to cover each of the 20 icosahedron faces, and actuated the skins to induce rolling locomotion (Fig. 6D).

In the above examples, the resulting robots performed comparably to purpose-built systems. For example, our tensegrity system moved at a speed of 0.06 body lengths per second (BL/s), compared with other six-bar tensegrity locomotion robots that have achieved 0.08 BL/s (*28*) and 0.05 BL/s (*29*). In calculating tensegrity body lengths, we divided the distance traveled over time by rod length, which represents a constant characteristic dimension for these robots. The wearable application we show with the robotic skins was able to mimic the functionality of the posture garments demonstrated in previous work (*30*–*32*) but was less integrated into the shirt, and the placement was not optimized for the biomechanics of each specific user. For our locomotion robots, the rowing robot locomoted at 0.6 BL/s (Fig. 4, C and D), the inchworm robot locomoted at 0.013 BL/s (Fig. 4, E and F), and the bodiless inchworm robot locomoted at 0.2 BL/s (Fig. 4, G and H). These speeds are comparable to purpose-built inchworm robots in the literature, which move between 0.014 BL/s (*33*) and 0.15 BL/s (*34*), as well as biological inchworms, which move between 0.28 and 0.62 BL/s, depending on the species (*35*). Body lengths reported here were measured as the length of the body in the direction of travel. This metric differs between fields, notably biology where the characteristic length between organisms varies by several orders of magnitude, and it is sometimes customary to measure body length as the longest length of the organism (*36*).

Our goal in making these comparisons is to demonstrate that the robotic skin concept can be used to produce robots with reasonable performance across a diversity of applications. The locomotion speeds reported herein are representative of rapidly prototyped systems, and better performance could be achieved through optimization, such as friction optimization between the robot and the surface. Further, there are trade-offs between optimization and design "on the fly" as related to force density: A purpose-built robot designed

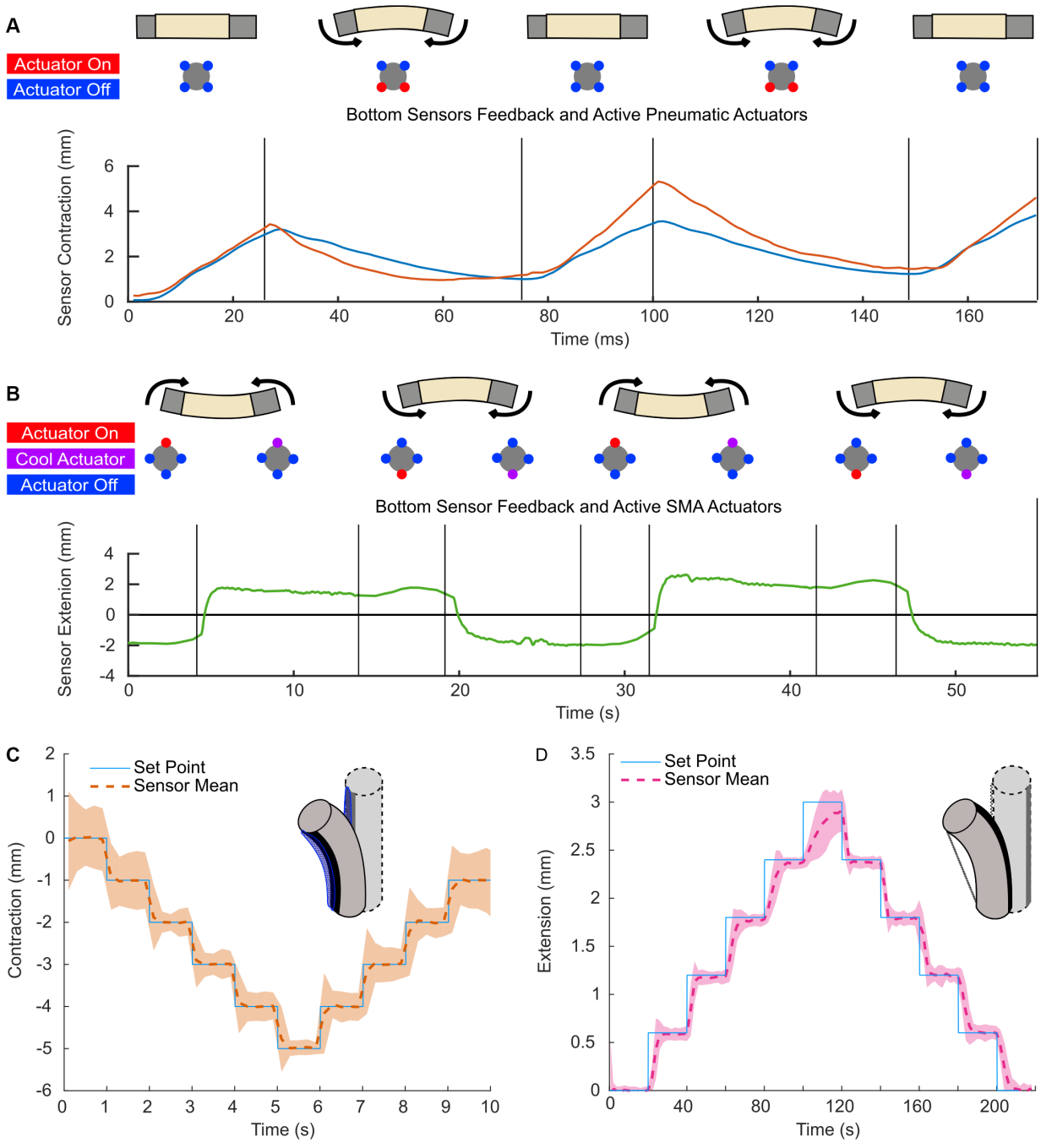

Fig. 5. Onboard sensors enable state feedback and closed-loop control of robotic skins. (**A** and **B**) Sensor feedback during open-loop locomotion for both pneumatic and SMA skins positioned on soft cylinders. Actuation sequencing is shown in the cross-section schematics. (**C** and **D**) The state feedback from the sensors may be used for closed-loop control of cylinder deflection. Solid lines indicate the set point, dashed lines indicate the mean position, and clouds indicate the 95% confidence interval, over multiple trials. Five trials are shown for the pneumatic skin and 10 trials are shown for the SMA skin.

for a single task (or finite collection of tasks) could likely use its body volume to produce greater forces, thereby potentially increasing efficiency but reducing multifunctionality. Our demonstrations emphasize a rapid design approach using reconfigurable robotic skins, allowing fewer materials and robots to be ported to accomplish a wide variety of tasks and, in some cases, retaining comparable function to their purpose-built counterparts.

DISCUSSION

Robotic skins produce motions by developing stresses within deformable bodies. The interaction between robotic skins and deformable bodies is complex and characterized by two related phenomena: the transfer of stress from the skin to the body and the resulting mechanical properties of the skin-body system. To effectively produce a deformation, the stresses developed within the skin

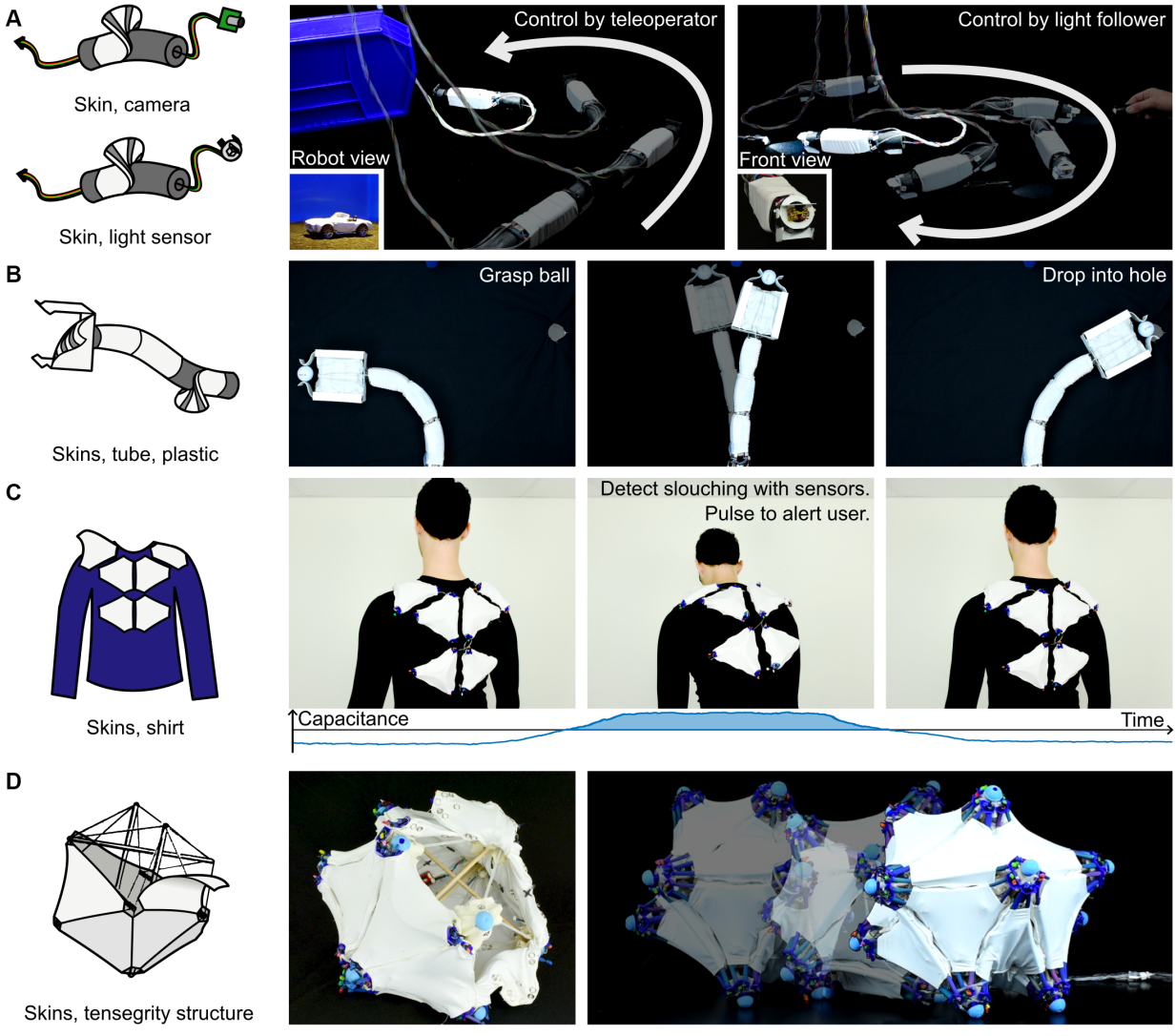

Fig. 6. Robotic skin demonstrations. (**A**) Inchworm locomotion robots include a camera for teleoperation or light sensors for light control, highlighting potential use cases in remote locations. (**B**) Three robotic skins around a soft cylinder form a continuum arm, and a fourth skin between two plates creates a gripper. This continuum manipulator moves a ball from one location to another. (**C**) Robotic skins attached to a garment detect poor posture and pulse to communicate with the wearer. (**D**) Twenty robotic skins covering the faces of a six-bar tensegrity generate membrane-driven locomotion.

by the actuators must be transferred into the body. Likewise, to accurately measure the state of the system, deformations in the body must be transferred back into the skin. If the body is too soft, loads will not be effectively transferred, and the skin will distort the surface of the body without producing bulk movements. If the body is too stiff, the skin will not generate sufficient stress to produce the required motion. The exact values of too soft and too stiff are highly dependent on the application and are under the control of the designer when selecting materials and morphologies.

The mechanical properties of the skin-body system are further influenced by skin design. In our implementations, both the sensors and the substrates are softer and thinner than the actuators, resulting in small contributions to the overall mechanical system. Rather, the mechanical properties of the skins are dominated by actuator choice and configuration, including alignment, areal density, and attachment scheme. There is a continuum of resulting skin-body properties that are available to the designer. At one extreme, for a large stiff body with few actuators sparsely populated within the skin, the system will exhibit properties similar to the body. At the other extreme, for a small soft body surrounded by a skin densely populated with actuators, the system will exhibit properties similar to the skin.

Modular, reconfigurable soft robots based on robotic skins have a number of advantageous features. (i) Robotic skins control deformable bodies from their surface, which allows robotic skins to turn passive, inanimate bodies into active soft robots. The robotic skin implementations presented here were able to create multiple stable system states with millimeter resolution when applied to inert deformable bodies. It is expected that with a set of dedicated deformable body designs and a more elaborate controller, higher precision could be achieved. (ii) They open the design space for soft robotics. Rather than designing a single, task-specific system, robotic skins enable on-the-fly design and production of many systems that perform a variety of functions. That is, in contrast to constructing 3D

soft robots with a tailored functionality, 2D robotic skins may be wrapped around 3D deformable bodies, removed, and then reoriented or transferred to other bodies to complete different tasks. Soft robots based on robotic skins can be quickly changed to adapt to changing system resources or requirements. For instance, the same robotic skins could be used to create robots that locomote, grasp, or manipulate objects, as we have demonstrated. (iii) This framework is independent of actuator, sensor, and material choice. As a result, the principles of design and actuation determined with one set of components will generalize well to other sets, regardless of application area. (iv) Robotic skins are 2D and may therefore be fabricated by using available printing and textile manufacturing methods. (v) They are compactable and may be stored flat, or folded and placed into a volume much smaller than their deployed size, making transportation easier. In addition, readily available deformable bodies that robotic skins may be positioned on, such as foam or inflatables, are also compactable and may consume very little volume during storage or transport. (vi) Systems generated by using robotic skins and deformable bodies continue to boast the attractive features of soft robots, such as lightweight and potentially low-cost materials; nonlinear motions resulting from simple controls; and damage resistance during impacts, falls, and vibrations. These features make soft robots more resilient and render them less sensitive to stressful mission environments. Robotic skins have these properties, along with the additional features of reconfigurability and multifunctionality. Therefore, we believe that this class of soft robots represents a step toward co-robotics and robot operation in the natural world, where different functions or gaits may be necessary to accommodate the demands of unpredictable and dynamic environments.

In this paper, we presented a new class of reconfigurable soft robots based on modular robotic skins that manipulate deformable soft bodies. We fabricated robotic skin prototypes using different materials and components, as well as different component geometries, to show the open design space for the robotic skin concept. We further provided concrete examples of how these skins can turn inanimate soft bodies into robots. For a given robotic skin, the motions that it can impart onto a soft body are a function of the material properties and morphology of that body (i.e., bulk modulus and stiffness), the orientation of the skin on the body, and the method of attachment or load transfer from the skin to the body. In this work, we have focused on the utilization of a small number of robotic skin prototypes to show how they interact with different bodies to achieve a variety of tasks. However, the basic concept of robotic skins is widely generalizable with different skin designs, different components, and different host bodies.

MATERIALS AND METHODS

Details for the fabrication and control of the robotic skins are provided in the Supplementary Materials. Briefly, elastomer-based robotic skins were composed of a silicone substrate with McKibben pneumatic actuators constructed with braided mesh and latex balloons adhered using tin-cure silicone (Mold Max 10) as a glue. Fabric-based robotic skins were composed of either coiled Nitinol SMA actuators or McKibben pneumatic actuators attached at their ends to a spandex substrate. All component combinations of robotic skins included high-deformation capacitive strain sensors made from conductive layers of EIG mixed with Dragon Skin 10 Slow Silicone and dielectric layers of Dragon Skin 10 Slow Silicone. The skins were controlled using logic controllers. We calculated robot speed resulting from different locomotion gaits as the distance traveled over time divided by the body length in the direction of travel. We quantified force-displacement characteristics of both the actuators and the soft bodies by using a materials tester. The theoretical basis for predicting surface-driven deformation of a soft cylinder, additional locomotion gaits, and examples of rapid prototyping with robotic skins are also provided in the Supplementary Materials.

SUPPLEMENTARY MATERIALS

robotics.sciencemag.org/cgi/content/full/3/22/eaat1853/DC1
Text S1. Actuators in robotic skin prototypes.
Text S2. Capacitive sensors and signal conditioning.
Text S3. Robotic skin construction.
Text S4. Predicting deformation of a known object.
Text S5. Predicting deformation of an unknown object.
Text S6. Control algorithms.
Text S7. Locomotion gaits using robotic skins.
Text S8. Rapid prototyping with robotic skins.
Fig. S1. McKibben actuator schematic.
Fig. S2. Capacitive sensor construction and characterization.
Fig. S3. Three robotic skin prototypes that vary in components, configuration, and integration.
Fig. S4. Force versus displacement curves for SMA/McKibben actuators and soft cylindrical bodies.
Fig. S5. A geometric model of a robotic skin deflecting a soft cylinder, with the neutral axis located along the surface of the cylinder.
Fig. S6. A geometric model of a robotic skin deflecting a soft cylinder, with the neutral axis located along the center of the cylinder.
Fig. S7. Control algorithms.
Fig. S8. Possible locomotion gaits using robotic skins with and without soft cylindrical bodies.
Fig. S9. Examples of rapid prototyping with robotic skins.
Movie S1. Transferability: continuum robots to locomotion robots.
Movie S2. Inchworm locomotion: teleoperated with camera.
Movie S3. Inchworm locomotion: controlled by light.
Movie S4. Continuum manipulation.
Movie S5. Wearable posture shirt.
Movie S6. Tensegrity ball rolling.
References (*37*–*39*)

REFERENCES AND NOTES

1. D. Rus, M. T. Tolley, Design, fabrication and control of soft robots. *Nature* **521**, 467–475 (2015).
2. C. Laschi, B. Mazzolai, M. Cianchetti, Soft robotics: Technologies and systems pushing the boundaries of robot abilities. *Sci. Robot.* **1**, eaah3690 (2016).
3. S. Kim, C. Laschi, B. Trimmer, Soft robotics: A bioinspired evolution in robotics. *Trends Biotechnol.* **31**, 287–294 (2013).
4. R. A. Bilodeau, R. K. Kramer, Self-healing and damage resilience for soft robotics: A review. *Front. Robot. AI* **4**, 48 (2017).
5. R. F. Shepherd, F. Ilievski, W. Choi, S. A. Morin, A. A. Stokes, A. D. Mazzeo, X. Chen, M. Wang, G. M. Whitesides, Multigait soft robot. *Proc. Natl. Acad. Sci. U.S.A.* **108**, 20400–20403 (2011).
6. F. Ilievski, A. D. Mazzeo, R. F. Shepherd, X. Chen, G. M. Whitesides, Soft robotics for chemists. *Angew. Chem. Int. Ed.* **50**, 1890–1895 (2011).
7. K. C. Galloway, K. P. Becker, B. Phillips, J. Kirby, S. Licht, D. Tchernov, R. J. Wood, D. F. Gruber, Soft robotic grippers for biological sampling on deep reefs. *Soft Robot.* **3**, 23–33 (2016).
8. Y.-L. Park, B.-r. Chen, C. Majidi, R. J. Wood, R. Nagpal, E. Goldfield, Active modular elastomer sleeve for soft wearable assistance robots, in *2012 IEEE/RSJ International Conference on Intelligent Robots and Systems (IROS)* (IEEE, 2012), pp. 1595–1602.
9. Y. Ding, M. Kim, S. Kuindersma, C. J. Walsh, Human-in-the-loop optimization of hip assistance with a soft exosuit during walking. *Sci. Robot.* **3**, eaar5438 (2018).
10. B. T. Quinlivan, S. Lee, P. Malcolm, D. M. Rossi, M. Grimmer, C. Siviy, N. Karavas, D. Wagner, A. Asbeck, I. Galiana, C. J. Walsh, Assistance magnitude versus metabolic cost reductions for a tethered multiarticular soft exosuit. *Sci. Robot.* **2**, eaah4416 (2017).
11. S. Seok, C. D. Onal, K.-J. Cho, R. J. Wood, D. Rus, S. Kim, Meshworm: A peristaltic soft robot with antagonistic nickel titanium coil actuators. *IEEE/ASME Trans. Mechatron.* **18**, 1485–1497 (2013).

12. M. T. Tolley, R. F. Shepherd, B. Mosadegh, K. C. Galloway, M. Wehner, M. Karpelson, R. J. Wood, G. M. Whitesides, A resilient, untethered soft robot. *Soft Robot.* **1**, 213–223 (2014).
13. J. Zou, Y. Lin, C. Ji, H. Yang, A reconfigurable omnidirectional soft robot based on caterpillar locomotion. *Soft Robot.* **5**, 164–174 (2018).
14. K. Kim, L.-H. Chen, B. Cera, M. Daly, E. Zhu, J. Despois, A. K. Agogino, V. SunSpiral, A. M. Agogino, Hopping and rolling locomotion with spherical tensegrity robots, in *2016 IEEE/RSJ International Conference on Intelligent Robots and Systems (IROS)* (IEEE, 2016), pp. 4369–4376.
15. Y. Sugiyama, A. Shiotsu, M. Yamanaka, S. Hirai, Circular/spherical robots for crawling and jumping, in *Proceedings of the 2005 IEEE International Conference on Robotics and Automation* (IEEE, 2005), pp. 3595–3600.
16. A. A. Stokes, R. F. Shepherd, S. A. Morin, F. Ilievski, G. M. Whitesides, A hybrid combining hard and soft robots. *Soft Robot.* **1**, 70–74 (2014).
17. S. W. Kwok, S. A. Morin, B. Mosadegh, J.-H. So, R. F. Shepherd, R. V. Martinez, B. Smith, F. C. Simeone, A. A. Stokes, G. M. Whitesides, Magnetic assembly of soft robots with hard components. *Adv. Funct. Mater.* **24**, 2180–2187 (2014).
18. S. A. Morin, Y. Shevchenko, J. Lessing, S. W. Kwok, R. F. Shepherd, A. A. Stokes, G. M. Whitesides, Using "click-e-bricks" to make 3D elastomeric structures. *Adv. Mater.* **26**, 5991–5999 (2014).
19. B. Holschuh, D. Newman, Two-spring model for active compression textiles with integrated NiTi coil actuators. *Smart Mater. Struct.* **24**, 035011 (2015).
20. M. Yuen, A. Cherian, J. C. Case, J. Seipel, R. K. Kramer, Conformable actuation and sensing with robotic fabric, in *2014 IEEE/RSJ International Conference on Intelligent Robots and Systems (IROS 2014)* (IEEE, 2014), pp. 580–586.
21. M. C. Yuen, R. A. Bilodeau, R. K. Kramer, Active variable stiffness fibers for multifunctional robotic fabrics. *IEEE Robot. Autom. Lett.* **1**, 708–715 (2016).
22. E. L. White, M. C. Yuen, J. C. Case, R. K. Kramer, Low-cost, facile, and scalable manufacturing of capacitive sensors for soft systems. *Adv. Mater. Technol.* **2**, 1700072 (2017).
23. R. J. Webster III, B. A. Jones, Design and kinematic modeling of constant curvature continuum robots: A review. *Int. J. Robot. Res.* **29**, 1661–1683 (2010).
24. A. Ghanbari, A. Rostami, S. M. R. S. Noorani, M. M. S. Fakhrabadi, Modeling and simulation of inchworm mode locomotion, in *Intelligent Robotics and Applications*, C. Xiong, Y. Huang, Y. Xiong, H. Liu, Eds. (Springer, 2008), pp. 617–624.
25. R. H. Plaut, Mathematical model of inchworm locomotion. *Int. J. NonLinear Mech.* **76**, 56–63 (2015).
26. J. Case, M. Yuen, M. Mohammed, R. Kramer, Sensor skins: An overview, in *Stretchable Bioelectronics for Medical Devices and Systems*, J. A. Rogers, R. Ghaffari, D.-H. Kim, Eds. (Microsystems and Nanosystems, Springer International Publishing, 2016), pp. 173–191.
27. J. C. Case, E. L. White, R. K. Kramer, Sensor enabled closed-loop bending control of soft beams. *Smart Mater. Struct.* **25**, 045018 (2016).
28. L.-H. Chen, B. Cera, E. L. Zhu, R. Edmunds, F. Rice, A. Bronars, E. Tang, S. R. Malekshahi, O. Romero, A. K. Agogino, A. M. Agogino, Inclined surface locomotion strategies for spherical tensegrity robots. arXiv:1708.08150 (2017).
29. A. P. Sabelhaus, J. Bruce, K. Caluwaerts, P. Manovi, R. F. Firoozi, S. Dobi, A. M. Agogino, V. SunSpiral, System design and locomotion of superball, an untethered tensegrity robot, in *2015 IEEE International Conference on Robotics and Automation (ICRA)* (IEEE, 2015), pp. 2867–2873.
30. Y. Zheng, J. B. Morrell, A vibrotactile feedback approach to posture guidance, in *2010 IEEE Haptics Symposium* (IEEE, 2010), pp. 351–358.
31. E. Sardini, M. Serpelloni, V. Pasqui, Daylong sitting posture measurement with a new wearable system for at home body movement monitoring, in *2015 IEEE International Instrumentation and Measurement Technology Conference (I2MTC) Proceedings* (IEEE, 2015), pp. 652–657.
32. C. Mattmann, O. Amft, H. Harms, G. Troster, F. Clemens, Recognizing upper body postures using textile strain sensors, in *2007 11th IEEE International Symposium on Wearable Computers* (IEEE, 2007), pp. 29–36.
33. S. M. Felton, M. T. Tolley, C. D. Onal, D. Rus, R. J. Wood, Robot self-assembly by folding: A printed inchworm robot, in *2013 IEEE International Conference on Robotics and Automation (ICRA)* (IEEE, 2013), pp. 277–282.
34. D. Lee, S. Kim, Y.-L. Park, R. J. Wood, Design of centimeter-scale inchworm robots with bidirectional claws, in *2011 IEEE International Conference on Robotics and Automation (ICRA)* (IEEE, 2011), pp. 3197–3204.
35. J. Brackenbury, Fast locomotion in caterpillars. *J. Insect Physiol.* **45**, 525–533 (1999).
36. N. Meyer-Vernet, J.-P. Rospars, How fast do living organisms move: Maximum speeds from bacteria to elephants and whales. *Am. J. Phys.* **83**, 719–722 (2015).
37. F. Daerden, D. Lefeber, Pneumatic artificial muscles: Actuators for robotics and automation. *Eur. J. Mech. Environ. Eng.* **47**, 10–21 (2002).
38. S.-M. An, J. Ryu, M. Cho, K.-J. Cho, Engineering design framework for a shape memory alloy coil spring actuator using a static two-state model. *Smart Mater. Struct.* **21**, 055009 (2012).
39. J. Case, J. Booth, D. Shah, M. Yuen, R. Kramer-Bottiglio, State and stiffness estimation using robotic fabrics, in *2018 IEEE International Conference on Soft Robotics (RoboSoft)* (IEEE, 2018), pp. 522–527.

Acknowledgments: We acknowledge A. Bottiglio for assistance with photography and media compilation. **Funding:** This work was primarily supported by the NASA through the Early Career Faculty Program (grant numbers NNX14AO52G and 80NSSC17K0553). D.S. was supported by the Air Force Office of Scientific Research under award number FA9550-16-1-0267 and by a NASA Space Technology Research Fellowship (grant number 80NSSC17K0164). J.C.C. was supported by a NASA Space Technology Research Fellowship (grant number NNX15AQ75H). E.L.W. and M.C.Y. were supported by NSF Graduate Research Fellowships (grant number DGE-1333468). **Author contributions:** R.K.-B. conceived the project, planned the experiments, and managed the research. J.W.B., D.S., E.L.W., M.C.Y., and O.C.-C. designed and built the hardware. J.W.B., D.S., J.C.C., and E.L.W. wrote the control algorithms. D.S. and J.C.C. developed the models. J.W.B., D.S., J.C.C., E.L.W., and O.C.-C. performed the experiments. J.W.B., D.S., and R.K.-B. drafted the manuscript. All authors contributed to, and agree with, the content of the final version of the manuscript. **Competing interests:** The authors declare that they have no competing interests. **Data and materials availability:** All data needed to evaluate the conclusions in the paper are present in the paper and/or the Supplementary Materials. Additional data related to this paper are available from the authors upon request.

Submitted 1 February 2018
Accepted 13 July 2018
Published 19 September 2018
10.1126/scirobotics.aat1853

Citation: J. W. Booth, D. Shah, J. C. Case, E. L. White, M. C. Yuen, O. Cyr-Choiniere, R. Kramer-Bottiglio, OmniSkins: Robotic skins that turn inanimate objects into multifunctional robots. *Sci. Robot.* **3**, eaat1853 (2018).

Science Robotics

OmniSkins: Robotic skins that turn inanimate objects into multifunctional robots

Joran W. Booth, Dylan Shah, Jennifer C. Case, Edward L. White, Michelle C. Yuen, Olivier Cyr-Choiniere and Rebecca Kramer-Bottiglio

Sci. Robotics **3**, eaat1853.
DOI: 10.1126/scirobotics.aat1853